

# Performance Evaluation of Photo Voltaic System with Quadratic Boost Converter Employing with MPPT Control Algorithms

K. Kumar \*, S. Rafi Kiran \*, T. Ramji \*\*‡, S. Saravanan \*\*\*, P. Pandiyan \*\*\*, N. Prabakaran \*\*\*\*

\*Department of EEE, SV College of Engineering, Tirupathi, India.

\*\*Department of EEE, Sri Krishna College of Engineering and Technology, Coimbatore, India.

\*\*\*Department of EEE, Sri Krishna College of Technology, Coimbatore, India.

\*\*\*\*School of Electrical and Electronics Engineering, SASTRA Deemed University, Thanjavur, India.

(kumar3kk@gmail.com, rafikiran@gmail.com, tiwariramis@gmail.com, saravanans087@gmail.com, pandyyan@gmail.com, prabaharan.nataraj@gmail.com)

‡

Ramji Tiwari, Department of EEE, Sri Krishna College of Engineering and Technology, Coimbatore – 641008, India, Tel: +91 8220818480, tiwariramjis@gmail.com

*Received: 16.04.2020 Accepted: 22.05.2020*

**Abstract-** This article explores the performance of the photovoltaic (PV) system with a quadratic boost converter (QBC) employing different MPPT control algorithms. The extraction of maximum power from high penetrating renewable energy sources (RES) and to step up the low voltage renewables into the desired voltage level with minimal power semiconductor switches are the foremost targets in the present renewable energy systems. Ample MPPT control techniques and power converter are available in the present research era. In this paper, the quadratic boost converter is premeditated for the analysis of the PV system with real-time data in the southern region of  $13^{\circ}39'29.3''N$   $79^{\circ}29'09.3''E$ . The quadratic boost converter has a higher voltage gain value with lower voltage stress and switching loss when compared with conventional boost converter. The efficacy of MPPT techniques in a 400 W PV system is evaluated by considering the P&O and ANFIS based MPPT controllers and the obtained results show the ANFIS based MPPT controller gives the best and stable output compared to the conventional P&O algorithm with real-time data in MATLAB/ Simulink environment.

**Keywords** High voltage gain; MPPT; PV System; Quadratic Boost Converter; Renewable sources.

## 1. Introduction

The rapid increase in the usage of fossil fuels in the power sector makes the concern about fossil usage and its effects on the present world environment conditions [1, 2]. As well known, the present research geared up towards the renewable green energy sources to identify the clean and cheap energy sources, by extract maximum energy from the available sources and to convert available low rated energy sources into the required energy level by using the advanced techniques in the power semiconductors [3].

From the literature, among all the renewable energy sources PV attained a special interest due to its abundant availability, clean and noiseless pollution-free operation. The power generation based on solar energy results in less voltage output. In order to improve this low voltage profile, there is a requirement for a variety of converter types as well

as Maximum Power Point tracking methods. In [4], the authors carried out a literature survey between the years 2010 to 2017 on the PV system with different MPPT techniques, the authors have also depicted the importance of extracting maximum power from the available renewable PV system. Similarly, a literature survey has been done in [5], to increase the voltage transfer conversion gain in the power electronic converters. The voltage conversion gain mainly depends on the usage of power semiconductor and reactive power components which is to be employed in the converter circuit design [6]. Each converter topologies have its own structure, gain values, efficiency and switching stress during the different operating duty cycle period [7].

Hill climb search (HCS) or perturb and observe (P&O) based MPPT technique is preferred when the optimum relation is known [8]. To track the optimum point in the P&O method is that by considering the varying the

maximizing variable constantly as well as observing the extracted power. Depending upon the acquired power variation along with perturbs operation, the successive size of the perturbation and direction is found until the technique achieves the optimum point. Generally, the dc-link components such as current and voltage are used as input to the control system whereas; the duty cycle is generated as output for the converter switch [9]. Thus, this reduces the system complexity and increases its dependability. The only setback of P&O algorithm is its convergence speed during variation in irradiance. During the variations in irradiance, the P&O system output will revolve around the MPP until the input system is being consistent [10].

The soft computing based MPPT strategy like a fuzzy logic controller (FLC) [11] and artificial neural network (ANN) are proposed to overcome the drawback of the P&O controller [12]. Soft computing strategies have better convergence speed and faster response during the changes in the irradiance and the temperature of the PV system. FLC based MPPT controller requires knowledge on system parameters in advance which makes the implementation complex process. The neural network is an enhanced controller which is used in non-linear systems to provide better stability. But the training of the neural network algorithm is complex. Hence, to overcome this ANFIS based MPPT technique is used which is the combination of FLC and NN. ANFIS strategy has quick response and simple implementation [13]-[15]. A detailed analysis of different MPPT techniques such as conventional, soft computing and hybrid techniques with their Advantages and disadvantages is presented [7].

The power electronic converter (PEC) is an essential component in the configuration of renewable based system [16]. The DC-DC converter is incorporated in the PV application to enhance the voltage based on the load requirement. The topology such as boost, buck-boost [2, 17], single-ended primary inductance converter (SEPIC) [18] and Cuk converter [18 - 20] are generally used for renewable application. Boost and buck-boost converter are the most basic converter topology. They have simple structure and cost-effective. But for high voltage application, the Boost converter fails for its high switching loss and voltage stress which reduces the overall efficient of the system [21, 22]. The QBC is proposed in this paper which works on the principle of two stage boost converter. The QBC have low switching loss and causes less stress on the switch by limiting the inrush current.

The aim of this paper is to analyze the performance of the PV system with QBC in MATLAB/Simulink by considering the real-time solar irradiation data in the region of 13°39'12.9" N 79°29'09.3" E. The effectiveness of the developed system is analyzed with constant irradiation data of 1000 W/m<sup>2</sup> at 25°C in standard test conditions and from the real time-varying irradiation data on March '19, September '19 and December '19. The output power obtained in all three time periods is compared and demonstrated with the MATLAB/Simulink results. Fig. 1 illustrates the 400 W PV systems with the high voltage

transfer gain QBC converter. The maximum power extracting duty cycle is derived from the ANFIS based MPPT controller.

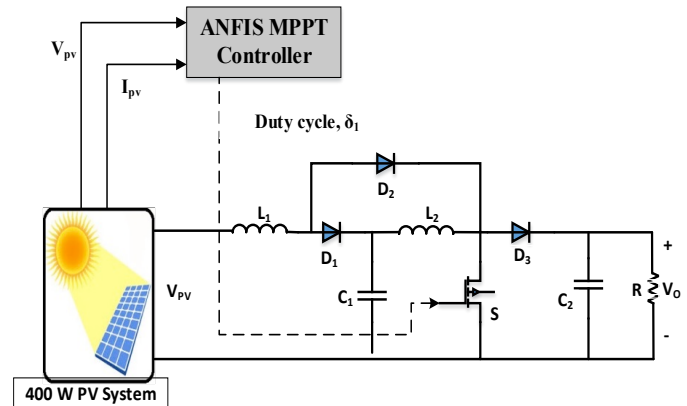


Fig. 1. Block diagram of the proposed system.

The paper is organized as follows; Section 2 represents the modelling of the PV system which is used in the proposed system. Section 3 describes the modelling of the quadratic boost converter and its parameters used for the proposed configuration. Section 4 explains the ANFIS based MPPT strategy and its structure. Section 5 illustrates the results of the proposed system by integrating with MATLAB/Simulink. Section 6 summarizes the findings of the proposed system.

2. Modelling of PV System

A PV system module consists of PV array which is arranged in series and parallel configuration to achieve the desired power. A single diode model of the PV system is shown in Fig. 2.

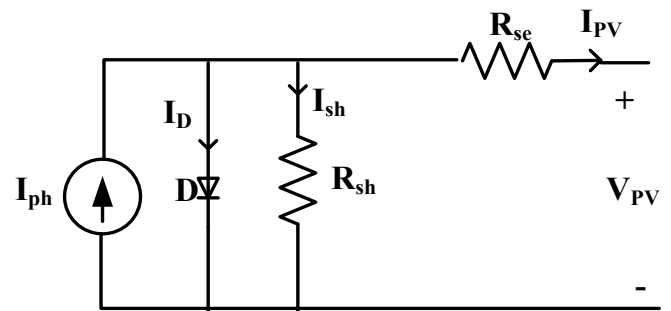


Fig. 2. Equivalent circuit of single diode PV cell

The output of the PV system depends on the specifications of the parameters of the PV module. In the proposed system, the Kyocera KD135GX-LP PV module is considered to design a 400 W PV system. The detailed parameter specifications of the PV module are listed in Table. 2. The output of the PV system relies on the solar irradiations and temperature. The mathematical modeling of the PV system is derived from the basic  $I_{pv}$ - $V_{pv}$  characteristics of the PV panel are as follows.

The output voltage ( $V_{pv}$ ) and output current ( $I_{pv}$ ) of PV system are defined as,

$$V_{pv} = \frac{\eta KT}{q} \ln\left(\frac{I_{ph}}{I_{pv}} + 1\right) \quad (1)$$

$$I_{pv} = I_{ph} - I_{pvsc} \left( e^{\frac{q(V_{pv} + I_{pv}R_s)}{\eta KT}} - 1 \right) - \frac{V_{pv} + I_{pv}R_{se}}{R_{sh}} \quad (2)$$

where,  $K$  is Boltzmann's constant ( $1.381 \times 10^{-23} \text{J/K}$ ) and  $q$  is elementary charge ( $1.603 \times 10^{-19} \text{C}$ ) Writing the shunt current as  $I_{pvsc} = (V + IR_s) / R_{sh}$ .  $R_{se}$ : series resistance ( $\Omega$ )  $R_{sh}$ : shunt resistance ( $\Omega$ ).  $I_{ph}$  represents Phase current ( $A$ ) and  $T$  represents Temperature ( $^{\circ}C$ ). The modelling parameters of PV system are available in literature for different irradiance and temperature [23]–[28].

### 3. Converter Analysis

The converter configuration of contemplated QBC for high voltage transfer gain in 400 W PV systems is shown in Fig. 3. It comprises of control switch  $S$ , three diodes of  $D_1$ ,  $D_2$  and  $D_3$ , two capacitors  $C_1$  and  $C_2$  and inductors of  $L_1$  and  $L_2$  with a load resistance of  $R$ .

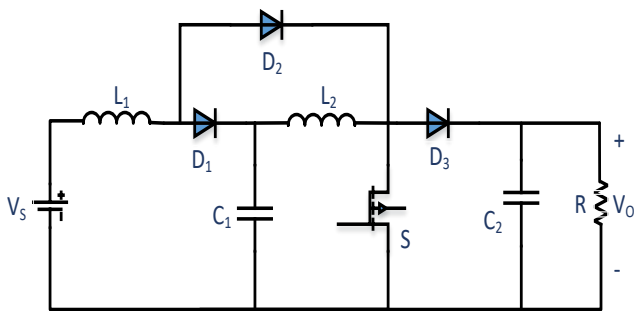


Fig. 3. Quadratic Boost Converter Topology

The voltage transfer gain of QBC is given in Eq. (3)

$$G = \frac{V_o}{V_s} = \frac{1}{(1-D)^2} \quad (3)$$

The modelling of parameters of QBC is as follows [2],

$$V_o = \frac{V_i}{(1-D)^2} \quad (4)$$

Where,  $V_o$  and  $V_i$  are the output voltage and input voltage respectively.  $D$  refers to the duty cycle.

The inductors are selected as follows,

$$L_1 = \frac{V_{i \min}}{2 * \Delta I_{L1} * f_s} * D \quad (5)$$

$$\Delta I_{L1} = \frac{I_o}{(1-D)^2} \quad (6)$$

$$L_2 = \frac{V_{i \min}}{2 * \Delta I_{L2} * f_s} * D \quad (7)$$

$$\Delta I_{L(n)} = \frac{I_o}{(1-D)} \quad (8)$$

The capacitors in QBC are selected as,

$$C_{dc} = \frac{I_o * D}{(1-D) \Delta V_{c1} * f_s} \quad (9)$$

$$V_{c1} = \frac{V_i}{(1-D)} \quad (10)$$

$$C_o = \frac{I_o * D}{\Delta V_{c2} * f_s} \quad (11)$$

$$V_{c2} = \frac{V_{c1}}{(1-D)} \quad (12)$$

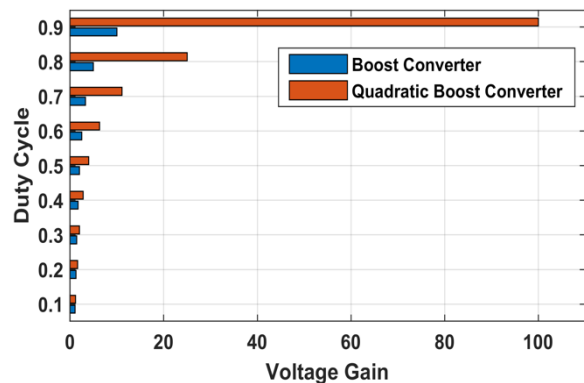


Fig. 4. Quadratic Boost Converter Voltage Transfer Gain

The voltage transfer gain of quadratic boost converter with different duty cycle ratio are presented in Fig. 4 and compared to the conventional Boost converter, the quadratic boost converter gives a maximum gain of 100, where as in conventional Boost converter gives a maximum of 10 voltage gain.

#### 3.1. Operating modes

**In Mode-I:** The control switch,  $S$  is in  $ON$  condition, then the diode  $D_2$  is in forward bias condition, whereas diodes  $D_1$  and  $D_3$  are in reverse bias condition. The current is supplied to inductors  $L_1$  and  $L_2$  by supplying voltage through a capacitor,  $C_1$  as represented in Fig. 5.

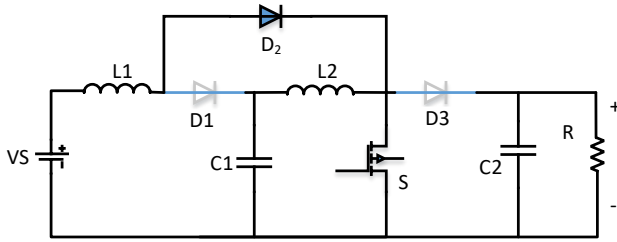


Fig. 5. QBC in Switch ON Condition

**In Mode-II:** The control switch, *S* is in OFF condition, then the diode, *D*<sub>2</sub> is in reverse bias and diodes *D*<sub>1</sub> and *D*<sub>3</sub> are in forward bias condition. The charging inductors *L*<sub>1</sub> and *L*<sub>2</sub> are in charging mode through the capacitors *C*<sub>1</sub> and *C*<sub>2</sub> respectively as represented in Fig. 6.

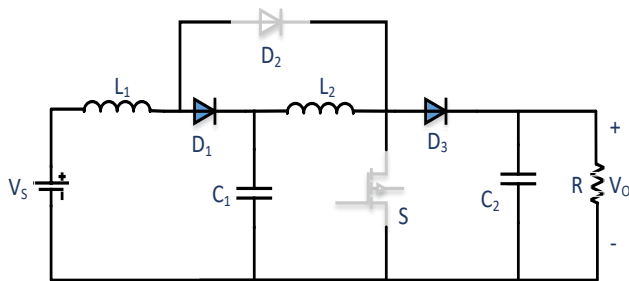


Fig. 6. QBC in Switch OFF Condition

The designed parameter values of QBC for 400 W PV system are listed in Table. 1.

Table 1. QBC Design parameters

Parameter Specifications	Values
Power Rating	400 W
Input voltage	18 V
Output Voltage	380 V
Switching frequency	20 kHz
Inductor, <i>L</i> <sub>1</sub>	4.3 mH
Inductor, <i>L</i> <sub>2</sub>	4.75mH
Capacitor, <i>C</i> <sub>1</sub>	17.23μF
Capacitor, <i>C</i> <sub>2</sub>	5.75 μF
Load resistor, <i>R</i>	358.4 Ω

4. ANFIS MPPT Controller

In literature, the maximum power extracting methods in a PV system are grouped into conventional, soft computing and hybrid methods. In conventional, the maximum power is extracted by using the methods hill-climbing, perturb and observer, incremental conductance methods, etc., these methods are simple in structure and easy to implement in the renewable PV system.

In the developed PV system, the maximum power is extracted by using the ANFIS MPPT controller to derive the operating duty cycle of the QBC converter [2]. ANFIS MPPT controller is a combination of fuzzy and neural

network. The combined feature of a single MPPT controller tracks the maximum power extracting duty cycle point in renewable energy source systems with high accuracy and speed.

4.1 ANN-ANFIS Training:

The number of layers considered for the proposed study is 5 as shown in Fig. 7. The transfer function model used is the sigmoid function. In the below equations *x*<sub>*i*</sub> is the *i*<sup>th</sup> input value; *w*<sub>*ij*</sub> is the weights assigned among the input and the hidden layer; *N* is the total number of input neurons; *w*<sub>*ki*</sub> is the weight among hidden and the output layer, and *k* is the number of output.

$$L_i = \sum_i^N x_i w_{ij} \tag{13}$$

$$M_i = \sum_i^N w_{ki} L_i \tag{14}$$

For the training of ANN, voltage and current inputs are considered in the hidden layer.

With two fuzzy if-then rules the formation of ANFIS data is explained in the following equations, which is derived from the T-S method of the fuzzy system.

if (*a* is *X*<sub>1</sub>) and (*b* is *Y*<sub>1</sub>) and (*d* is *Z*<sub>1</sub>)  
 then *f*<sub>1</sub> = *P*<sub>1</sub>*a* + *Q*<sub>1</sub>*b* + *z*<sub>1</sub> (15)

if (*a* is *X*<sub>2</sub>) and (*b* is *Y*<sub>2</sub>) and (*d* is *Z*<sub>2</sub>)  
 then *f*<sub>2</sub> = *P*<sub>2</sub>*a* + *Q*<sub>2</sub>*b* + *z*<sub>2</sub> (16)

One of the inputs given to the controllers is the output of the hybrid algorithm. The output from the ANFIS is given to the DC/DC converter.

The inputs to the ANFIS is a DC voltage and DC current control pulse.

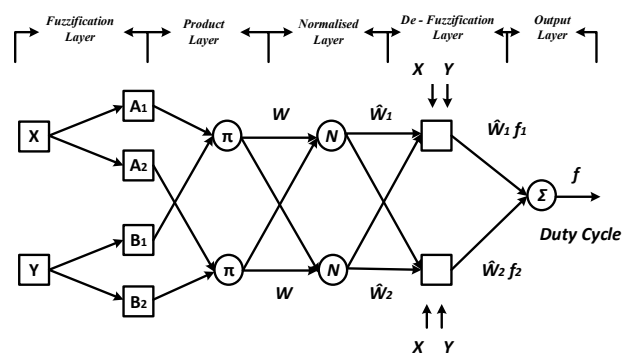


Fig. 7. Structure of ANFIS controller

The functions of 5 layers in the fuzzy inference system are provided below,

*Layer 1:* The nodes in the first layer is defined as a square node which is represented as,

$$\begin{aligned} N_{1,i} &= \mu_{X_i(a)} \text{ for } i = 1,2 \\ N_{1,i} &= \mu_{Y_i(b)} \text{ for } i = 3,4 \\ N_{1,i} &= \mu_{Z_i(c)} \text{ for } i = 5,6 \end{aligned} \quad (17)$$

*Layer 2:* The nodes present here are called circle nodes, which multiplies all inputs and provides a product output.

$$N_{2,i} = \phi_i = \mu_{X_i(a)}\mu_{Y_i(b)}\mu_{Z_i(c)} \quad (18)$$

*Layer 3:* The normalized firing strengths are calculated in the third layer circle nodes. The firing strength is calculated by using the successive relation.

$$N_{3,i} = \bar{\phi}_i = \frac{\phi_i}{\phi_1 + \phi_2} \quad (19)$$

*Layer 4:* These layers are defined as squared nodes defined with the function below,

$$N_{4,i} = \bar{\phi}_i f_i \quad (20)$$

*Layer 5:* This is the final layer in the structure, which is a circled node that provides a summation of all inputs forms the previous layer.

$$N_{5,i} = \sum_i \phi_i f_i \text{ (ANFIS)} \quad (21)$$

The rule system produces an optimum duty cycle in order to keep the dc bus voltage always constant and also to meet the load requirement in all weather conditions. The duty ratio of the bi-directional DC/DC converter is generated based on the rules and the input parameters.

There will be two inputs in the controller system and one output for ANFIS. This output is given to the PWM device then to the battery management system. Through this proposed method the DC link voltage is enhanced and also there will be a constant DC supply voltage.

In this paper, a developed 400 W PV system is analyzed with ANFIS MPPT controller and conventional P&O MPPT controller. The comparative performance results of the developed system with QBC converter output at the load side are compared.

### 5. Simulation Results and discussion

A 400 W PV system is designed in MATLAB/Simulink model by considering the Kyocera KD135GX-LP module

parameters datasheet as listed in Table 2. The proposed PV system with QBC along with the MPPT and PWM generator is modelled in the MATLAB/Simulink environment as shown in Fig. 8.

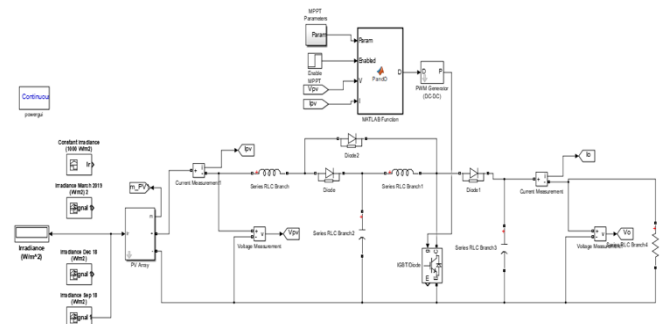


**Fig. 8.** Proposed Design and simulation of PV connected Quadratic boost converter

**Table 2.** PV System rating and specifications

PV Parameters	Specifications at STC
Module type	Kyocera KD135GX-LP
Series connected modules per string	1
Parallel strings	3
Open circuit voltage, $V_{oc}$	22.099 V
Short circuit current, $I_{sc}$	8.369 A
Voltage at maximum power point, $V_{mp}$	17.7 V
Current at maximum power point, $I_{mp}$	7.629 A
Series resistance, $R_s$	0.105 ohm
Parallel resistance, $R_p$	142.84 ohm
Saturation current, $I_{sat}$	$9.845e^{-7}$ A
Phase current, $I_{ph}$	8.37 A

In Fig. 9 it shows the Kyocera KD135GX-LP model 135 W PV system P-V and I-V characteristics and Fig. 10 shows the P-V and I-V characteristics of 400 W PV system, which is designed from the Kyocera KD135GX-LP module by connecting one series module per string and three strings in parallel.

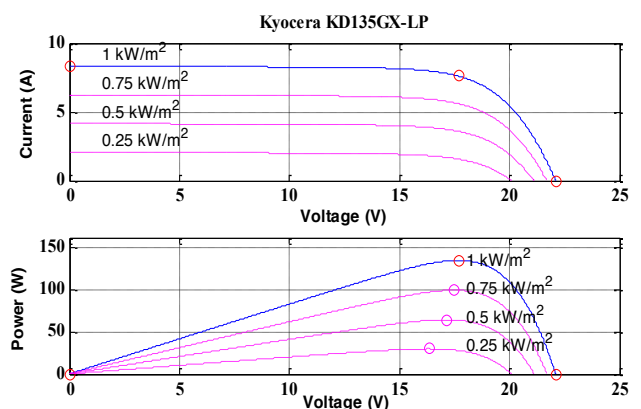


**Fig. 9.** 135 W PV system P-V and I-V characteristics of Kyocera KD135GX-LP.

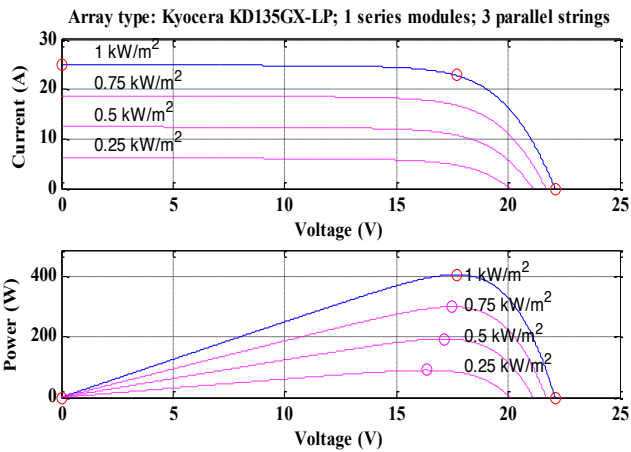


Fig. 10. 400 W PV system P-V and I-V characteristics of Kyocera KD135GX-LP.

In Fig. 11 it exhibits the 400 W PV system output with the output voltage of 17.7 V, current of 22.8 A and power of 400 W at standard test conditions. The output of the PV system is fed to QBC with ANFIS based MPPT controller, which gives the step-up the output voltage of 378 V, current of 1.01 A and 381.78 W power to the load, by operating converter duty cycle of 0.784 with a voltage gain of 21.4, which revealed in Fig. 12.

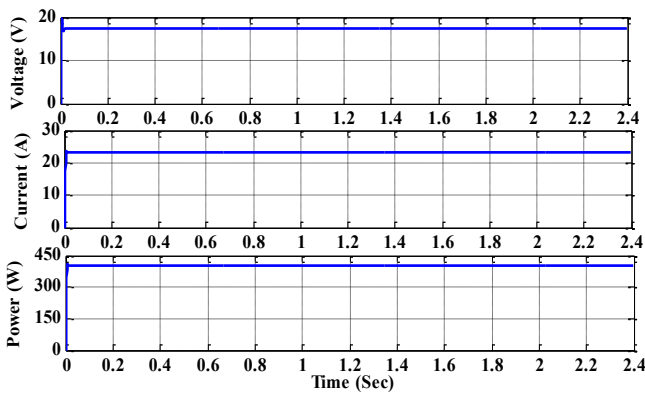


Fig. 11. Kyocera KD135GX-LP model PV system output voltage, current and power

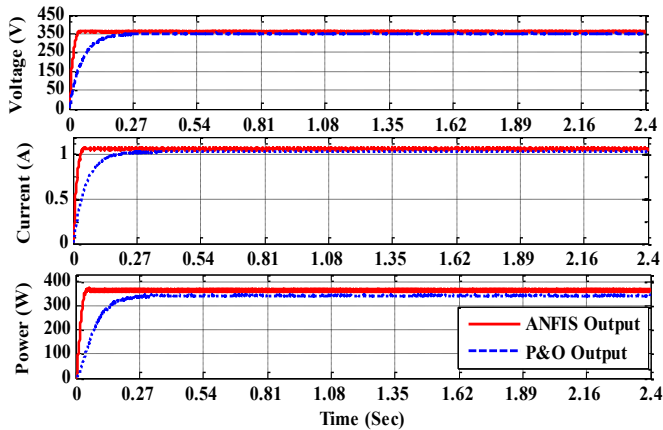


Fig. 12. PV system fed QBC converter output voltage, current and power

To evaluate the performance of the developed PV system, different solar irradiation data profiles along with humidity, module and ambient temperatures are considered in the region of 13°39'29.311"N 79°29'09.311"E in March '19, September '19 and December '19 which are presented in the Fig. 13 to Fig. 16 respectively. From the figures, it can be intercepted that the irradiance and temperature which is the main component for generation of power from PV system are non-linear in nature throughout the day and year too. It can be seen that the high irradiance and temperature can be obtained during time period of 1.00 PM to 4.00 PM. And in months March have higher production of power when compared from September and December months due to high irradiance and temperature value.

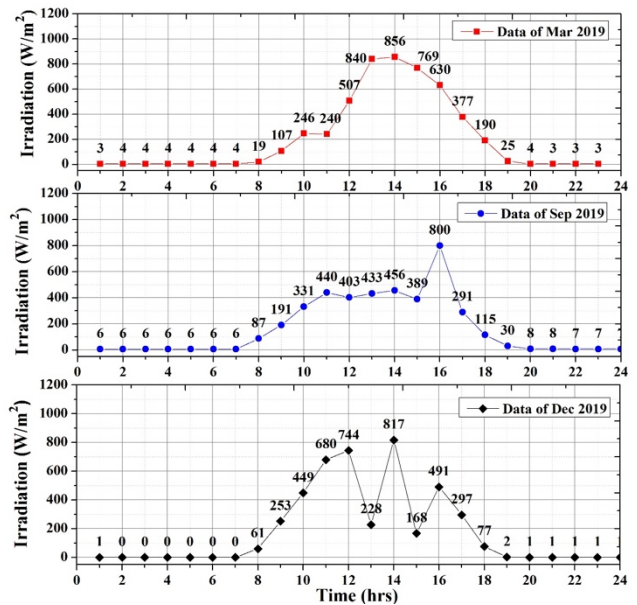


Fig. 13. Availability of Solar irradiation data on March '19, Sep '19 and Dec '19.

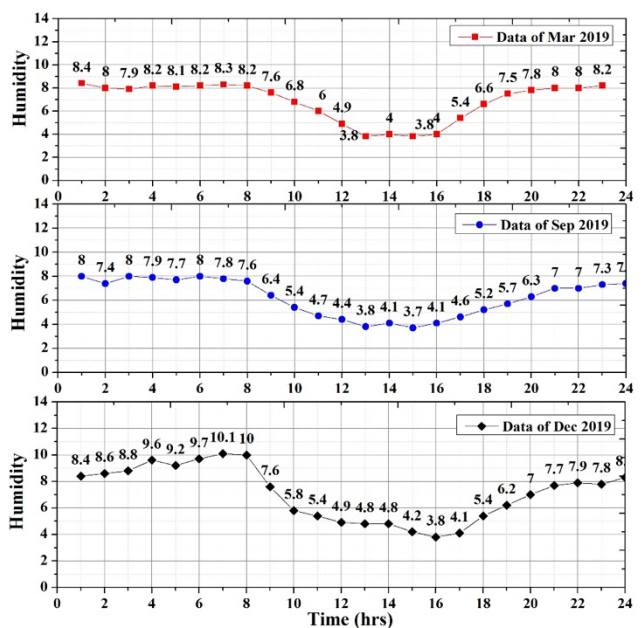


Fig. 14. Humidity data on March '19, Sep '19 and Dec '19.

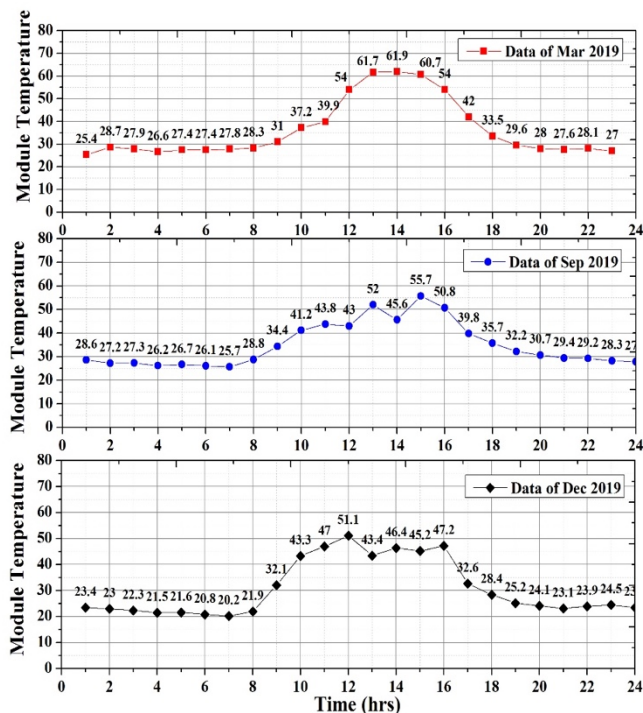


Fig. 15. Module temperature on March'19, Sep'19 and Dec'19.

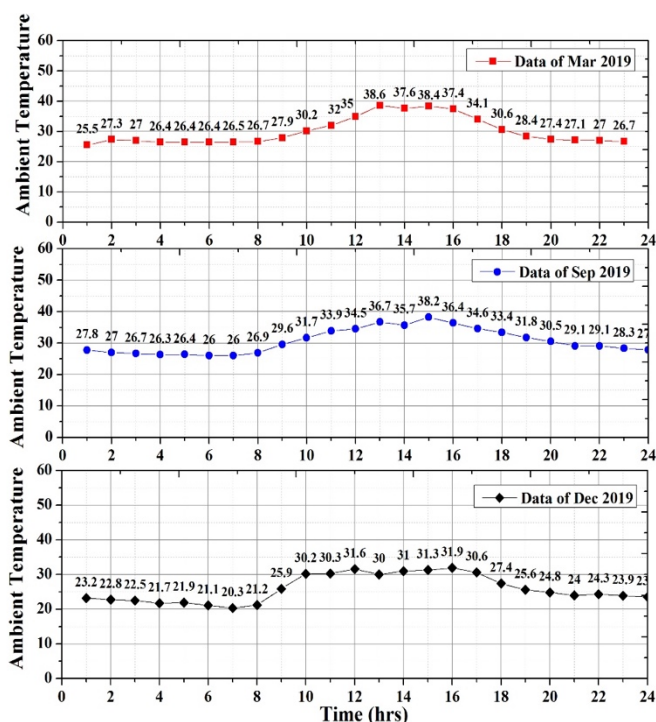


Fig. 16. Ambient temperature on March'19, Sep'19 and Dec'19.

The developed PV system with QBC output voltage, current and power profiles on March '19 are shown in Fig. 17 with respect to change in input weather data on March '19. Similarly, on September'19 and December '19 PV system output profiles of voltage, current and power are shown in Fig. 18 and Fig. 19 respectively.

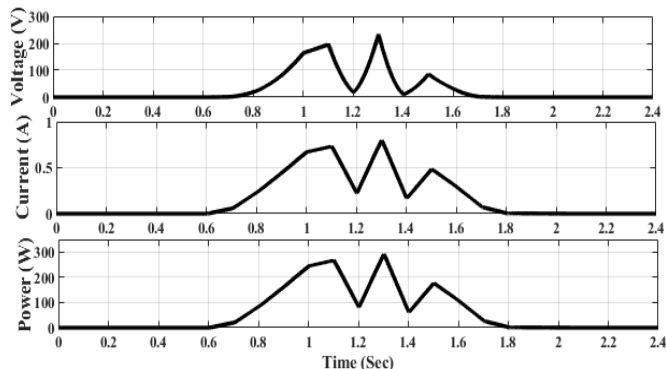


Fig. 18. PV system fed QBC converter output voltage, current and power on December 2019.

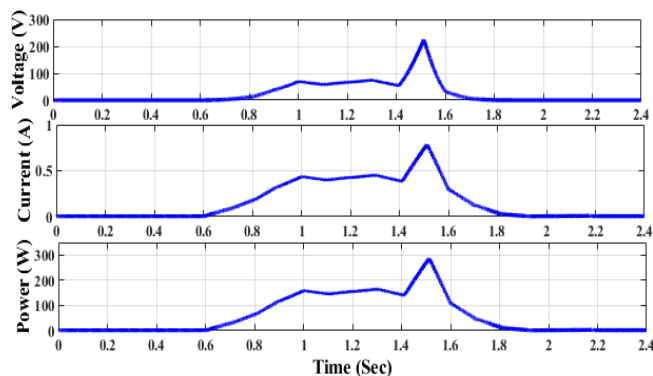


Fig. 19. PV system fed QBC converter output voltage, current and power on September 2019.

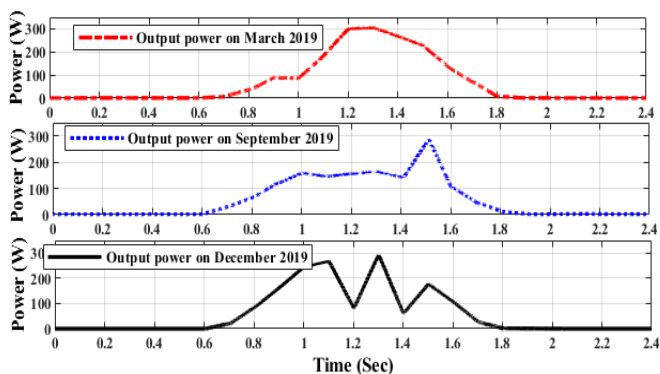


Fig. 20. Comparison of PV system fed QBC converter output power

In Fig. 20 the comparison of PV system fed QBC output power on all three considered weather condition profiles is illustrated. The output profile reveals that the output power of the PV system depends much on the solar irradiation and temperature data, as solar irradiation falling on the solar panels is disturbed by the environment cloudy condition in the sky. The obtained output power varies from time to time and on an average the maximum power is obtained for the period 12:00 to 13:00 noon. From March' 19 data, sudden drop and rise in power generation are observed in the system, which is due to the presence of clouds in the selected regions. As stated earlier, March produces more power than that of

September and December due to the availability of high irradiance and temperature for longer time. From, Fig. 20 it can depicted that the power generated in March' 19 during 12.00PM is 300 W which exist for longer time, whereas during September the 300 W can be achieved for lesser duration at 3.00 PM. During, December' 19 there is high fluctuation in the irradiance and temperature which causes the system to produce fluctuating power.

In Table 3 an analysis of power produced during time interval of 12.00 PM and 3.00 PM for better assessment is shown for three different months.

**Table 3.** Power rating for March' 19, September' 19 and December' 19 during 12.00 PM and 3.00 PM

Month/ Time Interval	March' 19	September' 19	December' 19
12. 00 PM	300 W	180 W	100 W
3.00 PM	215 W	300 W	190 W

## 6. Conclusion

In this paper, a 400 W PV system along with QBC is designed in MATLAB/Simulink environment. The performance of the developed system is analyzed by considering the P&O and NN based MPPT controllers under standard test conditions of 1000 W/m<sup>2</sup> and 25°C. The NN based MPPT controller proven the best result compared to the conventional P&O MPPT techniques. For the analysis of developed PV system with real-time data, the input weather conditions are taken in the region of 13°39'29.3"N 79°29'09.3"E on March '19, December '19 and September '18. The obtained power output results are compared and analyzed with conventional techniques. The proposed technique has a better stability and high voltage gain of about 10 with less voltage stress across the switch. From the results, the output power of the PV system depends much on the solar irradiation, humidity and temperature data on the PV panels.

## References

[1] K. Kumar, K. R. Prabhu, N. R. Babu, and P. Sanjeevikumar, "A Novel Six-Switch Power Converter for Single-Phase Wind Energy System Applications", *Advance. Smart Grid Renew. Energy- Lect. Notes Elect. Eng.*, Vol. 435, pp. 267-275, 2018.

[2] R. Tiwari, K. Krishnamurthy, R. B. Neelakandan, S. Padmanaban and P. W. Wheeler, "Neural Network based Maximum Power Point Tracking Control with Quadratic Boost Converter for PMSG - Wind Energy

Conversion System", *Electron.*, Vol. 7, No. 20, pp. 1-17, 2018.

[3] K. Kumar, S. R. Kiran, and A. Prasad, "Analysis of Solar Photovoltaic Source Fed BLDC Motor Drive with Double Boost Converter for Water Pumping Application in Irrigation System", *Int. J. Advance. Sci. Tech.*, Vol. 120, pp. 73-84, 2018.

[4] A. M. Eltamaly., H. M. H. Farh, and M. F. Othman, "A novel evaluation index for the photovoltaic maximum power point tracker techniques", *Solar Energy*, Vol. 174, pp. 940-956, 2018.

[5] H. Wang, A. Gaillard, and D. Hissel, "A review of DC/DC converter-based electrochemical impedance spectroscopy for fuel cell electric vehicles", *Renew. Energy*, Vol. 141, pp. 124-138, 2019.

[6] K. Kumar, N. R. Babu and K.R. Prabhu, , "Design and Analysis of RBFN-Based Single MPPT Controller for Hybrid Solar and Wind Energy System", *IEEE Access*, Vol. 5, pp.15308-15317, 2017.

[7] S. Saravanan, N. R. Babu, "Maximum power point tracking algorithms for photovoltaic system—A review", *Renew. Sustain. Energy Rev.*, vol. 57, pp. 192-204, 2018.

[8] R. Gules, W. M. Dos Santos, F. A. Dos Rei, E. F. Romaneli, and A. A. Badin, "A modified SEPIC converter with high static gain for renewable applications", *IEEE Trans. Power Electron.*, Vol. 29, No. 11, pp. 5860-71, 2013.

[9] Z. Chen, "PI and sliding mode control of a Cuk converter", *IEEE Trans. Power Electron.*, Vol. 27, No. 8, pp. 3695-703, 2012.

[10] T. Balamurugan, and S. Manoharan, "Fuzzy controller design using soft switching boost converter for MPPT in hybrid system", *Int. J. Soft Computing Eng.*, Vol. 2, No. 5, pp. 87-94, 2012.

[11] R. Kadri, J. P. Gaubert, G. Champenois, and M. Mostefaï, "Performance analysis of transformless single switch quadratic boost converter for grid connected photovoltaic systems", In *XIX Int. Conf. Elect. Mach.*, pp. 1-7, September 2010.

[12] S. Ozdemir, N. Altin, I. Sefa, "Fuzzy logic based MPPT controller for high conversion ratio quadratic boost converter", *Int. J. Hydrogen Energy*, Vol. 42, No. 28, pp. 17748-59, July 2017.

[13] R. K. Kharb, S. L. Shimi, S. Chatterji, and M. F. Ansari, "Modeling of solar PV module and maximum power point tracking using ANFIS", *Renew. Sustain. Energy Rev.*, Vol. 33, pp. 602-12, 2014.

[14] S. Benhalima, A. Chandra, and M. Rezkallah, "Real-time experimental implementation of an LMS-adaline-

- based ANFIS controller to drive PV interfacing power system”, IET Renew. Power Gen., Vol. 13, No. 7, pp. 1142-52, 2019.
- [15] T. V. Dixit, A. Yadav, S. Gupta, and A. Y. Abdelaziz, Power extraction from PV module using hybrid ANFIS controller, Solar Photovoltaic Power Plants, Springer, 2019, ch. 10.
- [16] H. K. Yadav, Y. Pal, and M. M. Tripathi, “A novel GA-ANFIS hybrid model for short-term solar PV power forecasting in Indian electricity market”, J. Inf. Optimization Sci., Vol. 40, No. 2, pp. 377-95, 2019.
- [17] K. Kumar, R. Tiwari, N. R. Babu, and K. R. Prabhu, “Analysis of MISO Super Lift Negative Output Luo Converter with MPPT for DC Grid Connected Hybrid PV/Wind System”, Energy Proc., Vol. 145, pp. 345-50, 2018.
- [18] K. Kumar, N. R. Babu, and K. R. Prabhu, “Design and analysis of an integrated Cuk-SEPIC converter with MPPT for standalone wind/PV hybrid system”, Int. J. Renew. Energy Res., Vol. 7, No. 1, pp. 96-106, 2017.
- [19] K. Krishnamurthy, S. Padmanaban, F. Blaabjerg, R. B. Neelakandan, and K. R. Prabhu, “Power Electronic Converter Configurations Integration with Hybrid Energy Sources—A Comprehensive Review for State-of-the-Art in Research”, Elect. Power Comp. Syst., Vol. 47, No. 18, pp. 1623-50, 2019.
- [20] K. Kumar, “Design and analysis of modified single P&O MPPT control algorithm for a standalone hybrid solar and wind energy conversion system”, Gazi Univ. J. Sci., Vol. 30, No. 4, pp. 296-312, 2017.
- [21] G. E. N. C. Naci, and D. Haji, “Dynamic Behavior Analysis of ANFIS Based MPPT Controller for Standalone Photovoltaic Systems”, Int. J. Renew. Energy Res., Vol. 10, No. 1, pp. 101-8, 2020.
- [22] S. A. M. Abdelwahab, A. M. Hamada, and W. S. Abdellatif, “Comparative Analysis of the Modified Perturb & Observe with Different MPPT Techniques for PV Grid Connected Systems”, Int. J. Renew. Energy Res., Vol. 10, No. 1, pp. 155-64, 2020.
- [23] R. Tiwari and N. R. Babu, "Fuzzy logic based MPPT for permanent magnet synchronous generator in wind energy conversion system." IFAC-PapersOnLine Vol. 49, No. 1, pp. 462-467, 2016.
- [24] K. Kajiwara, T. Kazuki, S. Ikeda, N. Matsui, and F. Kurokawa, "Performance Mechanism of Active Clamp Resonant SEPIC Converter in Renewable Energy Systems." 8th Int. Conf. Renew. Energy Res. and Appl., pp. 1042-1046, November 2019.
- [25] Y. Furukawa, H. Tomura, T. Suetsugu, and F. Kurokawa, "Variable Feedback Gain DC-DC Converter Tracing Output Voltage Fluctuation for Renewable Energy System." 8th Int. Conf. Renew. Energy Res. and Appl., pp. 916-921, November 2019.
- [26] K. C. Wijesinghe, "Optimized Integration of Solar PV Energy on to Telecom Power Systems for DC and A/C buses or Energy Storages with proposed Converters to make them as profit centers." 8th Int. Conf. Renew. Energy Res. and Appl., pp. 545-550, November 2019.
- [27] E. Kurt, and G. Soykan. "Performance Analysis of DC Grid Connected PV System Under Irradiation and Temperature Variations." 8th Int. Conf. Renew. Energy Res. and Appl., pp. 702-707, November 2019.
- [28] S. Marhraoui, A. Abbou, N. El Hichami, S. E. Rhaili, and M. R. Tur. "Grid-Connected PV Using Sliding Mode Based on Incremental Conductance MPPT and VSC." 8th Int. Conf. Renew. Energy Res. and Appl., pp. 516-520, November 2019.